fibers

MDPI

Article

Preparation, Characterization, and Surface Modification of Cellulose Nanocrystal from Lignocellulosic Biomass for Immobilized Lipase

Elvi Restiawaty [1,2,3], Neng Tresna Umi Culsum [3], Norikazu Nishiyama [4] and Yogi Wibisono Budhi [2,3,5,*]

[1] Department of Bioenergy Engineering and Chemurgy, Faculty of Industrial Technology, Institut Teknologi Bandung, Bandung 40132, Indonesia; erestiawaty@che.itb.ac.id
[2] Research Group of Chemical Engineering Process Design and Development, Institut Teknologi Bandung, Bandung 40132, Indonesia
[3] Department of Chemical Engineering, Faculty of Industrial Technology, Institut Teknologi Bandung, Bandung 40132, Indonesia; ntuculsum@students.itb.ac.id
[4] Division of Chemical Engineering, Graduate School of Engineering Science, Osaka University, 1-3 Machikaneyama-cho, Toyonaka 560-8531, Osaka, Japan; nisiyama@cheng.es.osaka-u.ac.jp
[5] Research Center of Nanoscience and Nanotechnology, Institut Teknologi Bandung, Bandung 40132, Indonesia
* Correspondence: y.wibisono@che.itb.ac.id

Abstract: This study reports the synthesis of cellulose nanocrystal (CNC) from sugarcane bagasse and rice straw as the matrix for immobilized lipase enzyme. The CNC surface was modified using cetyltrimethylammonium bromide (CTAB) to improve the interaction of CNC with glutaraldehyde so that CNC can immobilize lipase effectively. The results showed that after surface modification of CNC using CTAB with concentrations of 2–10 mM, the crystallinity of CNC slightly decreased. The presence of immobilized lipase on the modified CNC was confirmed visibly by the appearance of dark spots using transmission electron microscopy (TEM). The bond formed between the enzyme and CNC was approved using Fourier transform infrared spectroscopy (FTIR). FTIR results show a new amine group peak in the immobilized lipase, which is not present in the modified CNC itself. The modified CNC, both from bagasse (SB-20 A1-1) and rice straw (RS-20 B1-1), was successfully applied to the immobilized lipase enzyme with a yield of 88%. The observed free enzyme activity was 3.69 μmol/min·mL. The degree of hydrolysis of canola oil relative to free lipase (100%) from immobilized lipase at lipase SB-20 A1-1 and lipase RS-20 A1-1 was 23% and 30%, respectively. Therefore, this study successfully immobilized lipase and applied it to the hydrolysis of triglycerides.

Keywords: cellulose nanocrystal (CNC); hydrolysis; biomass; immobilization; lipase

Citation: Restiawaty, E.; Culsum, N.T.U.; Nishiyama, N.; Budhi, Y.W. Preparation, Characterization, and Surface Modification of Cellulose Nanocrystal from Lignocellulosic Biomass for Immobilized Lipase. *Fibers* **2022**, *10*, 33. https://doi.org/10.3390/fib10040033

Academic Editors: Tao-Hsing Chen and Shih-Chen Shi

Received: 22 November 2021
Accepted: 30 March 2022
Published: 2 April 2022

1. Introduction

The application of lipase as an enzyme in the hydrolysis processes opens an alternative method to reduce the energy consumption and thermal degradation of the product. Lipase has been widely used in various processes, such as oleochemical synthesis, pharmaceuticals, chemicals, and agrochemicals, and is also used in the production of renewable energy [1]. Lipase exhibits industrial potential and the ability to catalyze reactions, such as hydrolysis [1] and transesterification [2]. Some of the advantages of using lipase as a biocatalyst in fatty acid hydrolysis are high enzyme activity; mild reaction conditions (30–50 °C) leading to low energy consumption, and creating an environmentally friendly process. However, the enzymatic reactions using soluble enzymes are typically expensive, and it is difficult to regenerate and reuse the enzyme in these reactions [3]. To increase the lifetime of the enzyme in industry and reuse lipases, enzyme immobilization is performed in the buffer matrix [4]. Enzyme immobilization technology has been increasingly developing to improve the stability and reduce the separation and purification costs of the spent enzymes [1,2]. In particular, the immobilized enzymes in nanomaterial structure

showed high enzyme loading, increased mass transfer rates, and increased stability [5]. The characteristics of the buffer matrix can be porous or nonporous material, porous particles, nanoparticles, or membranes [6]. To reuse the enzyme after an operation, an immobilized enzyme on solid material is an attractive solution to overcome this problem. Currently, nanocellulose is a material that can be potentially used as matrix support for enzyme immobilization. Cellulose is a renewable biomaterial that has been widely studied because it exhibits superior properties, such as biocompatibility, biodegradability, stability, and low risk of environmental contamination [7]. A cellulose material that is derived from abundant amounts of naturally occurring polymers and is currently attracting attention is cellulose nanocrystal (CNC) [5,6,8–12]. CNC occurs in the form of rigid rod-like particles within length and width ranges of 100–250 nm and 5–70 nm, respectively [4]. Given that cellulose is a basic element for synthesizing CNC, agricultural waste represents a breakthrough as an interesting source due to its abundance, low cost, and widespread availability. Agriculture wastes generally consist of cellulose, hemicellulose, and lignin with chemical contents of 28–49 wt%, 15–32 wt%, and 4–26 wt%, respectively. The utilization of agricultural waste as feedstocks is attractive for CNC production because it provides the cheap raw material for the production of valuable nanomaterials [9]. The agricultural wastes that can be potentially utilized for CNC synthesis include rice straw and sugarcane bagasse because of their high cellulose concentrations. Hessien et al. [13] reported that rice straw contains 38 wt% cellulose, 32 wt% hemicellulose, 12 wt% lignin, and 18 wt% silica. Bagasse contains 45–50 wt% cellulose, 26 wt% hemicellulose, and 24 wt% lignin, as well as small quantities of ash and extractive substances [14].

CNC exhibits many interesting properties, such as low density (1.6 g/cm^3), high mechanical strength (modulus Young 100–140 GPa and tensile strength 7500 MPa), and high surface area (150–250 m^2/g). In addition, CNC also exhibits unique optical properties, low toxicity, biocompatibility, a high crystallinity index, and a low thermal expansion coefficient [15]. The presence of hydroxyl groups enables CNC to be easily modified by means of sulfonation, oxidation, ion exchange, and anhydrous acid [16,17]. This modification may represent a breakthrough for wide applications in catalytic engineering, enzyme immobilization, coating, and adhesives. Chitosan has been used as a material to modify the CNC surface such that it contains ammonium ions. In this study, CNC was synthesized using TEMPO ((2,2,6,6-Tetramethylpiperidin-1-yl)oxyl with the objective to modify its surface using cetyl trimethyl ammonium bromide (CTAB). Zainuddin et al. [18] have modified CNC using CTAB with the result that CTAB-CNC nanoparticles are able to bind large amounts of hydrophobic curcumin in drug delivery applications. In addition, Abitbol et al. [19] also performed a surface modification of CNC sulfate (CNC produced from the hydrolysis method) using CTAB. The results showed that modified with CTAB, CNC shows increased hydrophobicity. Compared with the original CNC, the CNC was more thermally stable and less hydrophilic after the surface modification reaction. In addition, the particle size and morphology of the CTAB-modified CNC remain unchanged.

The use of CTAB has several advantages in terms of low cost and its degradability by microorganisms [18,20]. In addition, the use of CTAB was necessary since the presence of this ion was expected to facilitate interactions with glutaraldehyde (GA) as a cross-linking agent for immobilized lipase. A supporting matrix is selected based on the characteristics needed to immobilize the enzyme, namely, mechanical strength, thermal stability, chemical stability, hydrophobic/hydrophilic functional groups, loading capacity, and costs [21]. Moreover, an alternative support matrix that is cheaper, nontoxic, and can immobilize enzymes more efficiently is ideal.

In this study, the CNC was modified by CTAB to improve the hydrophobicity of the CNC. The modification of CNC is expected to increase the interaction of CNC with glutaraldehyde so that CNC can immobilize lipase effectively. Therefore, the immobilized enzyme would be examined in the hydrolysis of vegetable oil. Previously, modification of CNC with CTAB for enzyme immobilization has not been reported, so the results of this study are expected to contribute significantly to the biocatalysts field. Furthermore, this

research utilized the agroindustry solid waste to produce the CNC, which was used as a support for enzyme immobilization in the hydrolysis process. The immobilized enzymes applied in the hydrolysis process can be used repeatedly.

2. Materials and Methods

2.1. Materials

The sugarcane bagasse (SB) and rice straw (RS) used in this research were obtained from Sumedang, West Java, Indonesia. Sodium hydroxide (NaOH), sodium bromide (NaBr), GA, and CTAB were purchased from Merck, Damstadt, Germany, while TEMPO and lipase enzyme where purchased from Sigma Aldrich, St. Louis, MO, United States. Sodium hypochlorite (NaOCl) solution was purchased from Avantor, Matsonford, USA. Distilled water was used in this experiment to prepare the solutions.

2.2. Alkali Pretreatment

The procedure of alkali pretreatment was performed as described by Isogai and Kato [21] with some necessary modifications. Briefly, the raw material, either SB or RS, was chopped into small pieces (80–120 mesh). Then, 20 g of raw material was loaded into a 160-mL batch reactor system and mixed with 20 wt% sodium hydroxide aqueous solution for 3 h at 30 °C. The ratio of the liquid to solid was set at 8 mL/g under continuous mechanical stirring at 300 rpm. After the reaction, the solid product was subsequently washed several times using distilled water until neutral, and the product was finally dried overnight. SB and RS that have received this alkaline treatment are referred to as SB-20 and RS-20, respectively.

2.3. Synthesis of CNC

The preparation of CNC using the TEMPO-mediated oxidation method was based on the procedure developed by Zhang et al. [7] with necessary modification. Briefly, 1 g of pretreated raw material (SB-20 or RS-20) was mixed with a 100 mL solution containing 0.1 g NaBr and 0.016 g TEMPO. Then, 5% NaOCl was added to the mixture to yield 7–11 mmol. The mixture was continuously stirred for 5 h at room temperature, and the pH of the solution was maintained at 10.0–10.5 by adding 0.5 M NaOH. Subsequent treatments of the solid product involved several washes using distilled water, centrifugation, and drying overnight. The SB-20 that had been converted to CNC using TEMPO and various amounts of NaOCl moles, i.e., 11, 9, and 7 moles, were coded as follows: SB-20 A1, SB-20 A2, and SB-20 A3, respectively. The same applied to RS-20, namely RS-20 B1, RS-20 B2, and RS-20 B3.

2.4. Surface Modification of CNC

The procedure of the surface modification of CNC followed Zainuddin et al. [18] with necessary modification. Here, 200 mg CNC (SB-20 A1 or RS-20 B1) was suspended in 50 mL distilled water, and 0.5 M NaOH solution was added to ensure that the CNC was well dispersed. The CNC suspension was gently added to the CTAB solution with concentrations varying from 2 to 10 mM. To maintain a homogeneous solution, the reacting system in the batch reactor was stirred at 300 rpm. The reaction was performed at 60 °C for 3 h. After completing this step, the solution was still stirred at room temperature overnight. The mixture obtained was then centrifuged for 10 min to remove the unreacted CTAB. The surface modification of SB-20 A1 using 2, 4, 6, 8, and 10 mM CTAB is then coded SB-20 A1-1, SB-20 A1-2, SB-20 A1-3, SB-20 A1-4, and SB-20 A1-5. A similar coding method was applied to the modified CNC of RS-20 B1 modification, namely RS-20 B1-1, RS-20 B1-2, RS-20 B1-3, RS-20 B1-4, and RS-20 B1-5.

2.5. Immobilization of Lipase on CNC Matrix

The immobilization process was conducted according to the procedure developed by Kim et al. [15] with necessary modifications. After surface modification, the modified CNC was mixed with 5% v/v GA for 5 h at 160 rpm and room temperature. The mixture was

washed using distilled water and dried in a desiccator before use. Thereafter, the modified CNCs were used to immobilize 0.1 mg/mL of lipase by incubating the mixture for 2 h at room temperature. The immobilized lipase was rinsed using phosphate buffer and stored at 4 °C. After the incubation was finished, the mixture was centrifuged. The supernatant was collected to determine immobilization yield using the Bradford method and expressed as the ratio of enzyme mass and support mass (mg lipase/mg CNC). The solid residue, which was immobilized lipase (Lipase SB-20 A1-1 or Lipase RS-20 B1-1), was washed with buffer phosphate solution (pH 7) to remove free lipase. The immobilization efficiency (%) was calculated via Equation (1) [22].

$$\text{Immobilization efficiency } (\%) = \frac{\text{Immobilized lipase}}{\text{total loading protein}} \times 100\% \quad (1)$$

2.6. Characterization

2.6.1. X-ray Diffraction

The crystallinity of the CNC product was examined using X-ray Diffraction (XRD) analysis. The X-ray diffractometer (Panalytical X'Pert-MPD) was operated with a CuK radiation of 1.542 Å, an electric current of 20 mA, and a voltage of 40 kV. The Crystallinity Index (CrI) of the CNC sample was calculated using the method of Segal et al. [23] as written in Equation (2).

$$\text{CrI } (\%) = \frac{I_{002} - I_{am}}{I_{002}} \times 100\% \quad (2)$$

I_{002} is the maximum intensity of the crystal plane (002) at diffraction around θ = 22°, and I_{am} is the intensity of amorphous (101) at diffraction around θ = 18°.

2.6.2. Transmission Electron Microscopy

The dimensions of the CNC were observed by using Transmission Electron Microscopy (TEM) (HT7700), operated at an accelerating voltage of 100 kV. The CNC suspension was dropped onto carbon-coated copper grids. Then, the staining reagent uranyless was dropped onto the grid and dried in the air.

2.6.3. Fourier Transform Infrared Spectroscopy

Fourier transform infrared spectroscopy (FTIR) was used to obtain the spectrum of sample functional groups. The samples were milled and mixed with KBr. The experiment was performed in the range of 500–4500 cm^{-1} with a resolution of 4 cm^{-1}.

2.6.4. Degree of Hydrolysis

The degree of hydrolysis (DH) was determined using Equation (3), which was previously used by Rooney and Weatherley [24].

$$\text{Degree of hydrolysis} = \frac{V_{NaOH} \times 10^{-3} \times M_{NaOH} \times Mr}{W_t \times f} \times 100\% \quad (3)$$

V_{NaOH} is the volume of NaOH needed to neutralize the sample in mL; M_{NaOH} is the concentration of NaOH solution, i.e., 0.1 M; Mr is the relative molecular mass of canola oil fatty acid (g/mol); W_t is the sample mass (g); and f is the mass fraction of oil in the mixture.

3. Results

3.1. Synthesis of Cellulose Nanocrystals

The synthesis of the CNC from sugarcane bagasse and rice straw was performed using the TEMPO method with alkali pretreatment as described by Isogai and Kato [21]. Visually, the results of this synthesis in the form of suspension (SB-20 A1, SB-20 A2, SB-20 A3, RS-20 B1, RS-20 B2, and RS-20 B3) are presented in Figure 1.

Figure 1. CNC products from (**a**) pretreated sugarcane bagasse (SB-20) and (**b**) pretreated rice straw (RS-20). The CNS synthesis from SB-20 using TEMPO and various moles of NaOCl, i.e., 11, 9, and 7 moles gives SB-20 A1, SB-20 A2, SB-20 A3, respectively, and RS-20 gives RS-20 B1, RS-20 B2, and RS-20 B3, respectively.

3.2. Thermogravimetric Analysis (TGA)

This analysis was used to observe the response of the CNC sample to temperature change. The performance curve of TGA is used to indicate the mass change during heating. Figure 2 shows thermal degradation, and a slight decrease of weight loss in the order of 10% occurred at a temperature of approximately 100 °C. At this temperature, the weight loss resulted from the evaporation of water. Profound weight loss occurs at temperatures from 200 to 500 °C, likely due to the occurrence of degradation of cellulose rings caused by breaking the glucosidic bonds [25,26].

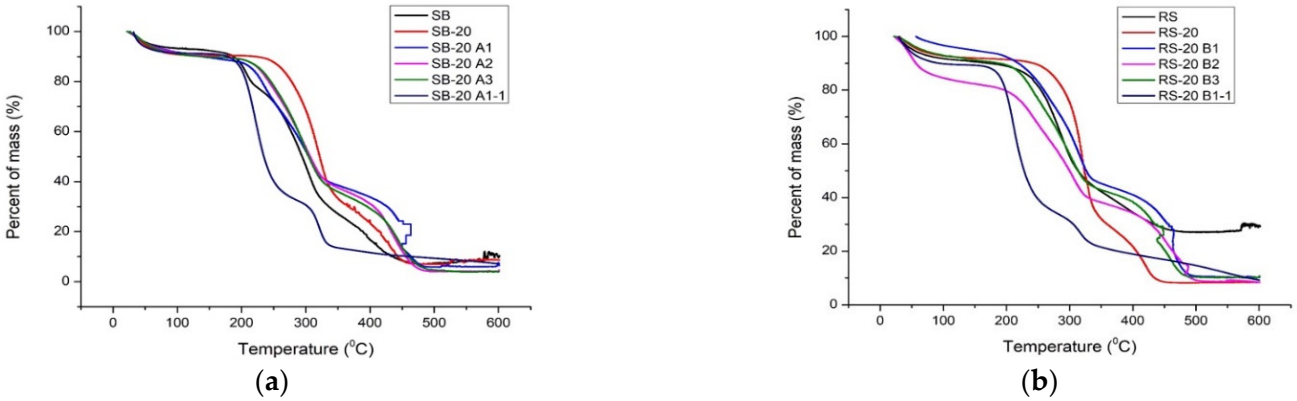

Figure 2. TGA of biomass, pretreated biomass using 20% NaOH, CNC synthesized with different concentration of NaOCl, and modified CNC from (**a**) sugarcane bagasse (SB) and (**b**) rice straw (RS).

3.3. Crystallinity of CNC

The XRD patterns of CNC produced from sugarcane bagasse and rice straw are shown in Figure 3. Based on the XRD measurement, the CNC diffraction peaks appear at 15.1, 17.5, and 22.7°, representing the typical diffraction peaks of cellulose I with crystals planes (110), ($1\bar{1}0$), and (200), respectively [26]. According to Chindaprasirt and Rattanasak [27] and Zhang et al. [28], the XRD peaks that appear at 20.9 and 26.6 come from crystalline silica in the form of quartz. Table 1 shows the crystallinity of CNC from sugarcane bagasse (SB) and rice straw (RS) before and after TEMPO treatments.

The XRD patterns of CNC after surface modification using various concentrations of CTAB are presented in Figure 4, while the crystallinity of CNC from sugarcane bagasse (SB) and rice straw (RS) are shown in Table 2.

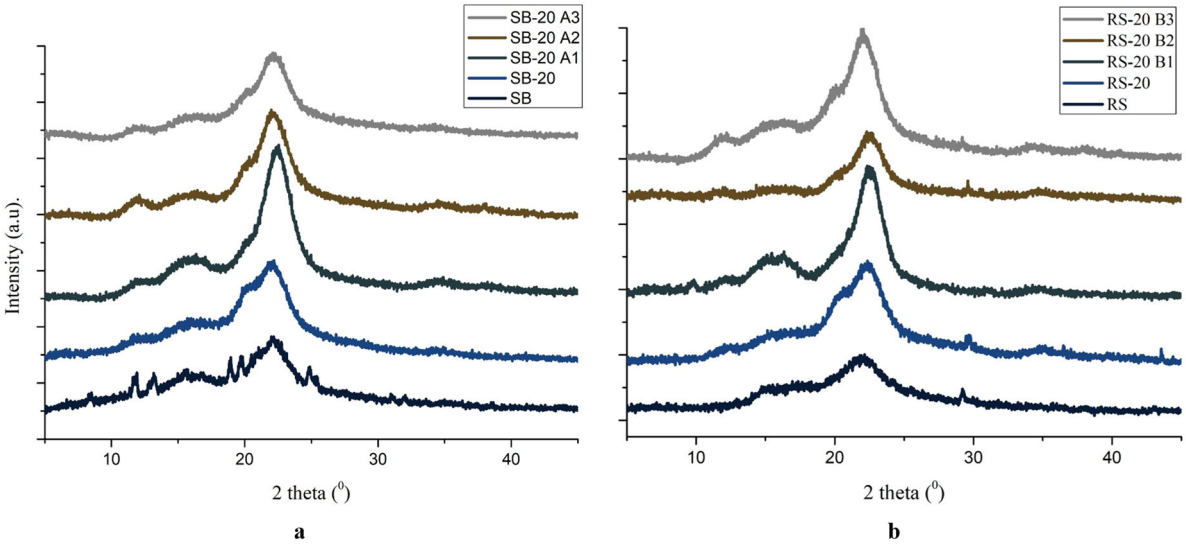

Figure 3. X-ray diffraction patterns of the biomass, the alkaline pretreated biomass, and the CNC from (**a**) sugarcane bagasse (SB), (**b**) rice straw (RS). The number "20" in the sample code indicates that the sample has been pretreated with 20% NaOH. The letters A and B refer to samples from sugarcane bagasse and straw, respectively. The last digit in the CNC sample code indicates a different concentration of NaOCl. 1 = 11 mM NaOCl; 2 = 9 mM NaOCl; and 3 = 7 mM NaOCl.

Table 1. Crystallinity of CNC from sugarcane bagasse (SB) and rice straw (RS).

No	Sample Code	Details	CrI (%)
1	SB	Raw materials of sugarcane bagasse	56
2	SB-20	SB after pretreatment using 20% NaOH	65
3	SB-20 A1	SB-20 oxidized with TEMPO and 11 mmol NaOCl	80
4	SB-20 A2	SB-20 oxidized with TEMPO and 9 mmol NaOCl	77
5	SB-20 A3	SB-20 oxidized with TEMPO and 7 mmol NaOCl	76
6	RS	Raw materials of rice straw	56
7	RS-20	RS after pretreatment using 20% NaOH	72
8	RS-20 B1	RS-20 oxidized with TEMPO and 11 mmol NaOCl	86
9	RS-20 B2	RS-20 oxidized with TEMPO and 9 mmol NaOCl	85
10	RS-20 B3	RS-20 oxidized with TEMPO and 7 mmol NaOCl	74

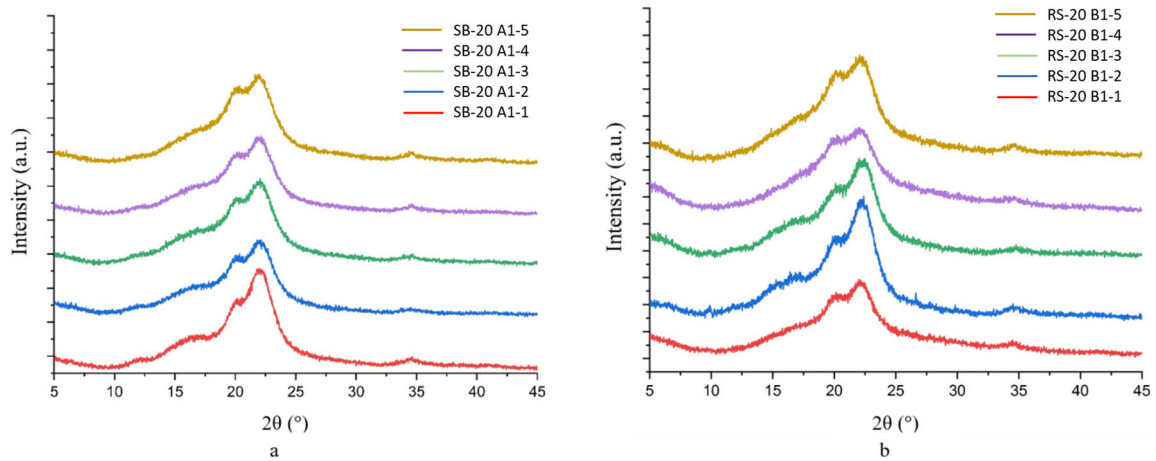

Figure 4. X-ray diffraction patterns of CNC from (**a**) sugarcane bagasse (SB-20 A1) and (**b**) rice straw (RS-20 B1) after surface modification with various concentrations of CTAB. The last digit in the modified CNC sample code indicates a different CTAB concentration. 1 = 2 mM CTAB; 2 = 4 mM CTAB; 3 = 6 mM CTAB; 4 = 8 mM CTAB; and 5 = 10 mM CTAB.

Table 2. Crystallinity of the modified CNC using CTAB from sugarcane bagasse (SB) and rice straw (RS).

No	Sample Code	Details	CrI (%)
1	SB-20 A1-1	Modification of SB-20 A1 using 2 mM CTAB	69
2	SB-20 A1-2	Modification of SB-20 A1 using 4 mM CTAB	66
3	SB-20 A1-3	Modification of SB-20 A1 using 6 mM CTAB	63
4	SB-20 A1-4	Modification of SB-20 A1 using 8 mM CTAB	62
5	SB-20 A1-5	Modification of SB-20 A1 using 10 mM CTAB	62
6	RS-20 B1-1	Modification of RS-20 A1 using 2 mM CTAB	62
7	RS-20 B1-2	Modification of RS-20 A1 using 4 mM CTAB	63
8	RS-20 B1-3	Modification of RS-20 A1 using 6 mM CTAB	66
9	RS-20 B1-4	Modification of RS-20 A1 using 8 mM CTAB	60
10	RS-20 B1-5	Modification of RS-20 A1 using 10 mM CTAB	61

3.4. Morphological and Dimensional Analysis of CNC

To support the visual analysis as previously discussed, morphological and dimensional analyses using TEM were performed to determine the effect of modified CNC by NaOCl and CTAB on morphology and particle size. The results of morphological analysis through TEM are presented in Figure 5 for sugarcane bagasse and rice straw.

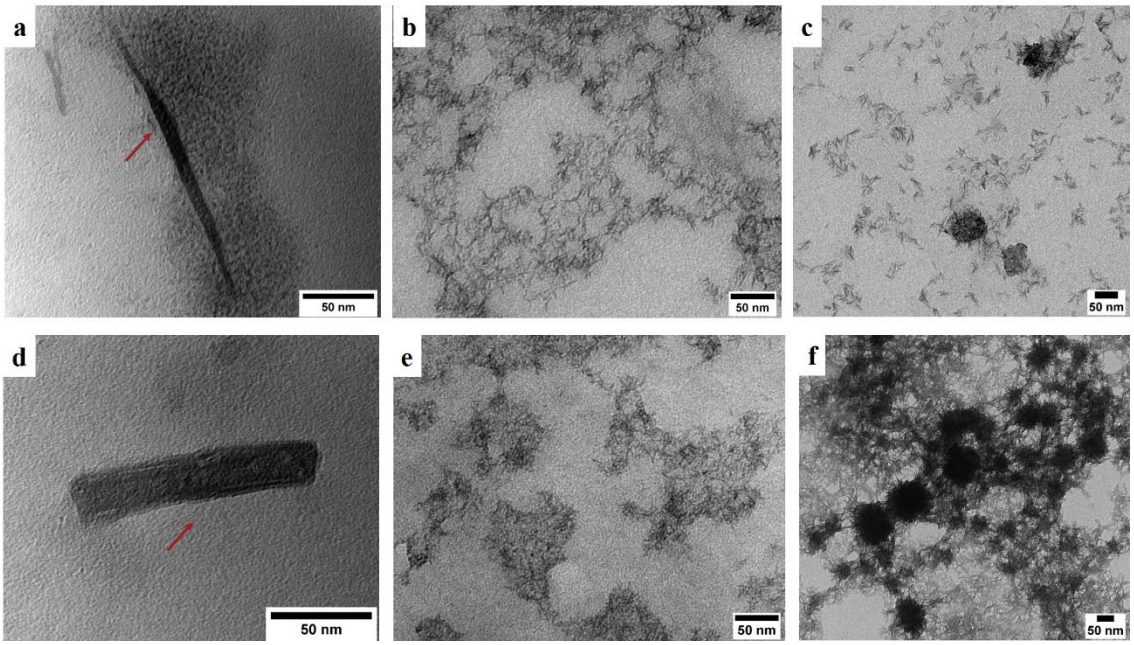

Figure 5. TEM images for (**a**) CNC from sugarcane bagasse (SB-20), (**b**) the modified SB-20 A1-1, (**c**) Immobilized lipase (Lipase SB-20 A1-1), (**d**) CNC from rice straw (RS-20), (**e**) the modified RS-20 B1-1, and (**f**) Immobilized lipase (Lipase RS-20 B1-1).

3.5. Fourier Transform Infrared Spectroscopy

The result of the Fourier transform Infrared Spectroscopy (FTIR) spectra of the CNC is shown in Figure 6. This characterization was used to identify the functional groups of the sample produced.

3.6. Degree of Hydrolysis

The activity of immobilized lipase in the modified CNC was examined using canola oil as the substrate to confirm that the functionality of the enzyme was working properly. The activity of free and immobilized lipase was compared. Figure 7 depicts the activity of enzymes immobilized on modified CNC derived from bagasse (SB-20) and rice straw (RS-20) relative to free enzymes. The free enzyme exhibits higher activity compared with immobilized enzymes. The enzyme immobilized on SB-20 A1-1 had the best activity compared with other

immobilized enzymes SB-20; meanwhile, the enzyme-immobilized RS-20 B1-1 had the highest activity compared with other immobilized enzymes SB-20 and RS-20.

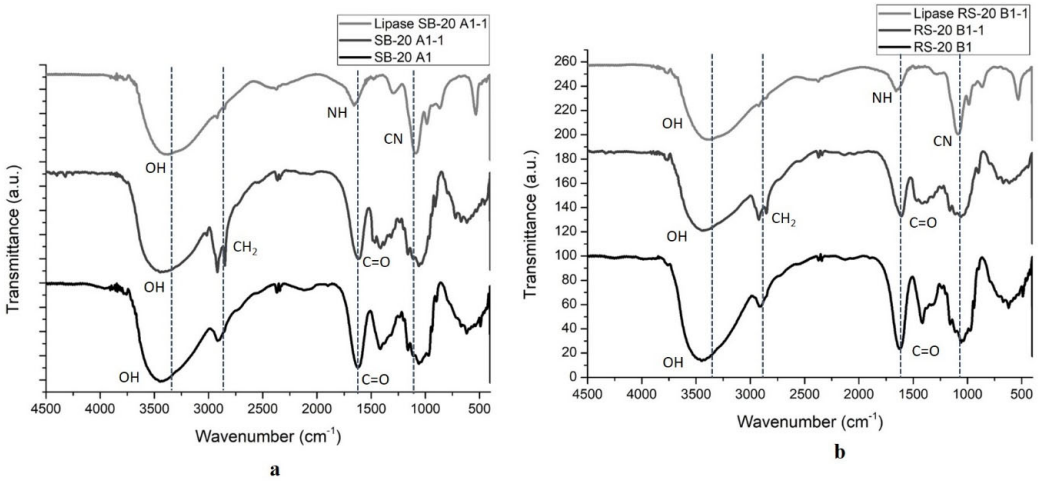

Figure 6. FTIR spectra of unmodified CNC, modified CNC, and the immobilized lipase: (**a**) unmodified CNC (SB-20 A1) and modified CNC (SB-20 A1-1) from sugarcane bagasse, and immobilized lipase (Lipase SB-20 A1-1); (**b**) unmodified CNC (RS-20 B1) and modified CNC (RS-20 B1-1) from rice straw and immobilized lipase (Lipase RS-20 B1-1).

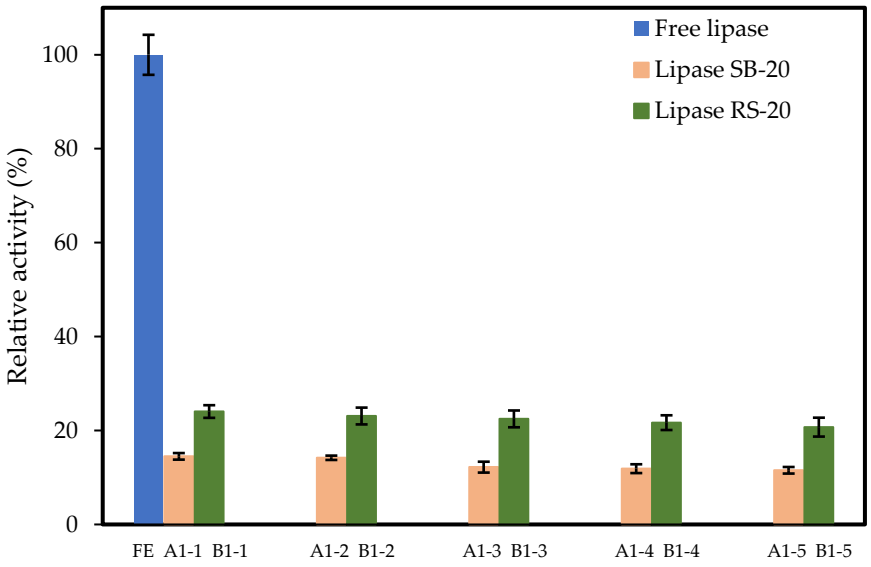

Figure 7. The activity of immobilized enzymes in various CNC modifications was relative to the activity of free enzymes. Activity testing was carried out at a temperature of 25 °C.

The efficiency of the immobilized enzymes in the CNC matrix can be seen in Table 3. Lipase RS-20 B1-1 showed higher immobilization efficiency (86.63% ± 2.41) than lipase SB-20 A1-1 (82.98% ± 7.5). As a result, the lipase activity of RS-20 B1-1 gave higher activity than lipase SB-20 A1-1.

Table 3. Enzyme activity of the free and immobilized enzyme and immobilization efficiency of lipase on immobilized enzyme using canola oil.

No.	Biocatalyst	Activity (U/mg-Enzyme)	Immobilization Efficiency (%)
1	Free lipase	1.04 ± 0.09	-
2	Lipase SB-20 A1-1	0.26 ± 0.01	82.98 ± 7.50
3	Lipase RS-20 B1-1	0.16 ± 0.01	86.63 ± 2.41

The activities of immobilized lipase on the modified CNC and free lipase were tested at hydrolysis temperatures of 30 to 50 °C to assess their thermal stability (see Figure 8). Free lipase performs very well at a temperature of 30 °C. Free lipase activity decreased significantly with increasing temperature. At a temperature of 50 °C, the free lipase activity was reduced by 51.6% from the free lipase activity at 30 °C. Lipase activity of RS-20 B1-1 was higher than that of lipase SB-20 A1-1 in the temperature range of 30–50 °C. Both immobilized enzymes showed the highest activity at a temperature of 40 °C. Increasing the temperature to 50 °C only decreased the activity of about 2.6% and 6.1% of lipase SB-20 A1-1 and lipase RS-20 B1-1, respectively.

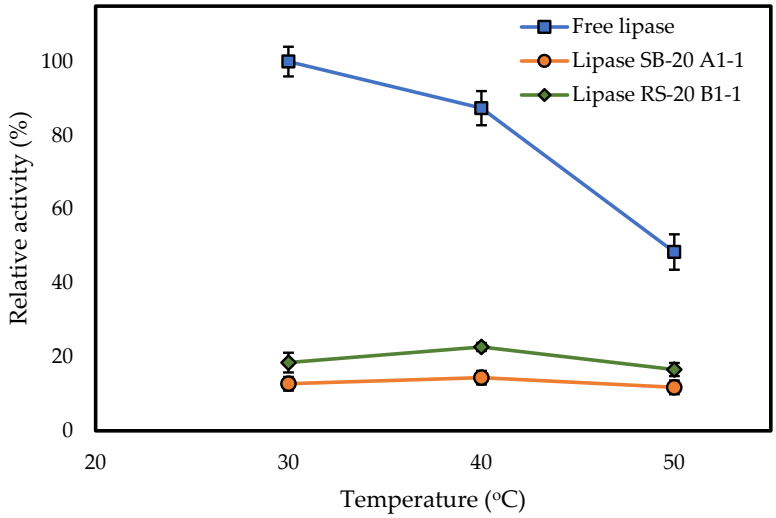

Figure 8. Effect of hydrolysis temperature on the enzyme activities of lipase SB-20 A1-1 and lipase RS-20 B1-1 relative to free lipase activity. Hydrolysis was carried out for 2 h.

The degrees of hydrolysis of the immobilized enzyme during hydrolysis of canola oil and soybean oil are presented in Figure 9. The results showed that free enzymes had greater activity than immobilized enzymes (lipase SB-20 A1-1 and RS-20 B1-1), both for hydrolysis of canola oil and hydrolysis of soybean oil. The degree of hydrolysis of canola oil and soybean oil using SB-20 A1-1 were (21.4 ± 1.9)% and (9.8 ± 2.8)%, respectively. Meanwhile, the degree of hydrolysis of canola oil and soybean oil using RS-20 B1-1 were (28.5 ± 1.4)% and (12.3 ± 2.7)%, respectively.

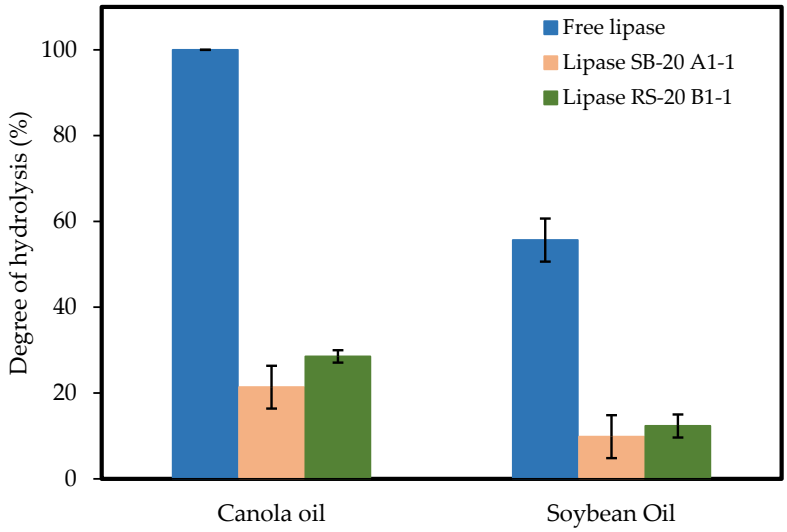

Figure 9. Comparison of hydrolysis degree for free enzyme and immobilized lipase on sugarcane bagasse (SB-20 A1-1) and rice straw (RS-20 B1-1). Hydrolysis was carried out at 40 °C for 6 h.

A comparison of research results with several previous studies is presented in Table 4. Based on the comparison with the results of other studies, the degree of immobilized hydrolysis is lower than that of the free enzyme. However, the concentration of the enzyme (U/mL-substrate or U/g-substrate) and the operating conditions used can affect the difference in the degree of hydrolysis.

Table 4. Comparison with the previous studies.

Enzyme	Enzyme Source	Support	Substrate	Enzyme Concentration	Time	Degree of Hydrolysis	Ref.
Free lipase	*Ricinus communis*	-	canola oil	81.3 ± 0.29 U/g-substrate	3 h	88%	[29]
Free lipase	*C. rugosa*	-	olive oil	200 U/g-substrate	24 h	98%	[30]
Free lipase	*C. rugosa*	-	canola oil	3.69 ± 0.29 U/mL-substrate	6 h	100%	this work
Immobilized lipase RS-20 B1-1	*C. rugosa*	cnc	canola oil	0.75 ± 1.16 U/mL-substrate	6 h	30%	this work
Immobilized lipase	*C. cylindracea*	activated carbon	jatropha oil	4.03 U/mL-substrate	3 h	78%	[31]
Immobilized lipase	*C. rugosa*	amberlite IRC-50	olive oil	300 U/g-substrate	24 h	91%	[30]

3.7. Reusability of Immobilized Lipase

The reusability of immobilized lipase on sugarcane bagasse (SB) and rice straw (RS) for canola oil hydrolysis was performed to investigate the stability of lipase when it was repeatedly used. The data on reusability for sugarcane bagasse and rice straw are presented in Figure 10.

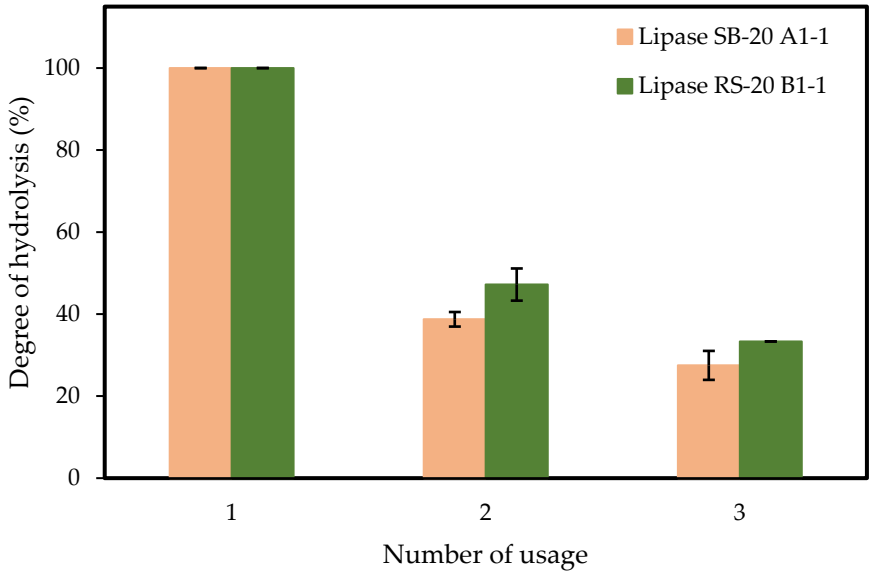

Figure 10. Comparison of reusability in terms of hydrolysis degree for immobilized lipase on sugarcane bagasse (SB-20 A1-1) and rice straw (RS-20 B1-1).

4. Discussion

Based on Figure 1, the addition of NaOCl affected the suspension color of CNC significantly for both raw materials. Increasing the moles of NaOCl from 7 mmol to 11 mmol resulted in a whiter CNC solution for SB-20 and RS-20. This phenomenon can be explained as follows: By increasing the NaOCl concentration during the reaction, the removal of noncellulose components and other impurities, such as lignin, hemicellulose, and pectin, became easier. The white color of the CNC solution observed in the reaction product indicated that a significant amount of cellulose material was produced. The results obtained in this study are consistent with research conducted by Johar et al. [32], which explains that the color of the raw materials changes from brown to white after chemical treatment. These visual results were used as guidance or initial screening to select which run required further confirmation.

As indicated in Figure 2, to investigate the thermal degradation, a decrease in mass at approximately 10% was noted due to H_2O evaporation over the surface. The evaporation of intermolecular H bonds in water occurred at approximately 120 °C in all samples. Significant degradation of the CNC sample occurs at 200–300 °C. A comparison of the degradation temperature of the raw material and the pretreated material reveals that the degradation temperature of the raw material sample is low because of the presence of lignin, hemicellulose, and noncellulose material decomposed at low temperatures. For CNC samples, the thermal degradation at low temperatures with a wider range shows lower thermal stability due to the smaller nanoparticle size and long chain [33,34]. The results of TGA measurements after CTAB modification showed similar curves to SB and RS before and after treatment, where there was a slight decrease in weight at a temperature of around 100 °C due to evaporation of water. For surfactant-modified CNC, two prominent weight loss peaks were observed around 250–300 °C, which were attributed to the degradation of the surfactant chain and CNC carboxylate groups. The second degradation occurs at a temperature of around 325 °C, which is related to the dissociation of the CNC crystal structure [35].

Based on the results of XRD measurements (Figure 3) and the crystallinity, as shown in Table 1, the sugarcane bagasse exhibits a crystallinity of 56%. However, after alkali pretreatment using 20% w/v NaOH solution, the crystallinity of the raw material increases to 65%. The crystallinity of the pretreated sugarcane bagasse increases due to the decay of the amorphous part of the raw material. This finding is consistent with the results of research conducted by Knill and Kennedy [36], which states that NaOH solutions can penetrate the crystallites and damage the hydrogen bonds (inter and intra) between cellulose molecules and the surrounding crystalline regions. Thus, the crystallinity of CNC has increased. The treatment of cellulose molecular chains in the presence of NaOH can cause damage to the structure of cellulose I, which is then converted into cellulose II. At higher NaOH concentrations, Na+ ions can penetrate the structure and cause swelling. Crystal swelling is the beginning of the polymorphic transformation of cellulose Iβ to cellulose II [37,38]. Some or even all lignin can dissolve in NaOH solution, and the hemicellulose fraction can be degraded, depending on the experimental conditions.

The CNC produced from the sugarcane bagasse using the TEMPO oxidation method with 7–11 mmol NaOCl exhibits different levels of crystallinity, spanning from 76% to 80% (see Figure 3). CNC crystallinity increases as a function of oxidation concentration. As the oxidation concentration increases, the number of amorphous sites that are attacked also increases. This finding is consistent with the research of Cao et al. [39], reporting an increase in crystallinity after TEMPO oxidation due to the loss of part of the amorphous region. The existence of the NaOCl in the solution during TEMPO oxidation played an important role in destroying the amorphous region. This CNC crystallinity value confirms that the product has reached the minimum requirement for CNC. A similar behavior could be observed for the synthesis of CNC from rice straw. Specifically, the crystallinity of the raw material was only 56% and increased to 72% after alkali pretreatment. Increasing the moles of NaOCl during the CNC synthesis resulted in increased CNC crystallinity.

CNC from sugarcane bagasse or rice straw with the highest crystallinity (SB-20 A1 and RS-20 B1) was then used for surface modification using CTAB. The detailed modifications of the SB-20 A1 and RS-20 B1 are given in Table 2. As a result, the XRD patterns of CNC after surface modification are shown in Figure 4. After surface modification, the crystallinity of the CNC produced from sugarcane bagasse and rice straw showed a slight decrease, as shown in Table 2. For CNC from sugarcane bagasse, increasing the CTAB concentration from 2 to 10 mM reduced CNC crystallinity from 69% to 62%, while the CNC from sugarcane bagasse without surface modification (SB-20 A1) had a crystallinity of 80%. However, for CNC from rice straw, the reduction of crystallinity was irregular by increasing CTAB concentration from 2 to 10 mM. Overall, all variations of CTAB concentrations exhibited that the crystallinity is still above the minimum CNC crystallinity value, i.e., 54% [40]. The surface modifications of CNC using CTAB could change the crystalline

portion due to the attachment of the large structure of the long alkyl chain of CTAB, which might slightly enlarge the amorphous portion of the modified CNC [18]. The cellulose modification could affect the cellulose component as it could disrupt the cellulose crystal structure during the modification process, thus decreasing crystallinity [41]. The surface modification and CTAB attachment to CNC could convert the crystalline portion to a disordered state. Zainuddin et al. [18] performed research on surface modification of CNC, and the results revealed a slight difference in CNC diffractogram after modification using CTAB. In addition, Xiang et al. [42] and Nagalakshmaiah et al. [43] reported that modified CNC using CTAB did not affect the crystallinity of CNC because CTAB modification is mainly on the surface.

Based on Figure 5a,d, the CNC from sugarcane bagasse has a type of rod-like morphology with a length of 215 ± 83 nm, and CNC morphology from rice straw shows a rod-like type with an average length of 103 ± 23 nm. The morphology and dimension of CNC produced from the hydrolysis of β-1,4-glucosidic bonds in the amorphous zone randomly resulted in fibers with shorter diameters and lengths [44]. CNC morphology depends on several factors, such as raw material, operating condition during the reaction (reaction time, concentration, temperature), and method (oxidation, hydrolysis) [45]. After CNC modification using CTAB (Figure 5b,e), CNC from bagasse and CNC from rice straw showed the same results. CNC surfaces have a rod-like morphology, and after modification, the morphology was changed to become scattered and distorted because of aggregation. This phenomenon occurs because the CTAB can generate the surface hydrophilicity of the particles to differ [42]. Figure 5c,f shows the presence of lipase immobilized on CNC. Lipase, which is a macromolecule, can cause an increase in thickness in the morphology of CNC, which is indicated by the presence of thick black lumps. The presence of lipase also causes buildup due to differences in the size of the lipase molecules that bind to the CNC. Zhu et al. (2014) reported that TEM results showed several bright spots of PPL that were observable and indicated that the metal nanoparticle (MNP) surface was covered by enzymes [46].

Based on Figure 6, the peak at 1246 cm^{-1} indicates the presence of a C-H group. Moreover, the peaks that appear at 3444, 2916, and 1056 cm^{-1} show the stretching vibrations of O–H, C–H, and C–O from cellulose, respectively [47]. The peak at 1680 cm^{-1} arises from the carbonyl group that appears due to the TEMPO-mediated oxidation of CNCs. Interestingly, after surface modification using CTAB, the IR spectrum of CNC product results in a new peak at 2850 cm^{-1}, indicating the presence of an asymmetric CH_2 group of alkyl chains [35]. In addition, the peak that appears at 1483 cm^{-1} shows the rocking vibration of the CH_2 group [18]. Based on FTIR characterization, it showed that immobilized lipase onto CNCs become a resulting new peak at 1294 cm^{-1} (lipase SB-20 A1-1) and 1280 cm^{-1} (lipase RS-20 B1-1) from functional group C–N and peak at 1658 cm^{-1} (lipase SB-20 A1-1) and 1654 cm^{-1} (lipase RS-20 B1-1) from functional group N–H [48]. Thus, modified CNC using GA has proven that it can immobilize lipase enzymes.

According to the results of FTIR characterization, TEMPO-oxidized CNC (named unmodified CNC) contains a carboxyl group on its surface. The enzyme immobilization process in CNC consists of five steps (see Figure 11). Before surface CNC modification, the COOH group of unmodified CNC was converted to the COO^- group through deprotonation (step 1). After that, surfactant cation was adsorbed to the resulting COO^- group through electrostatic interactions (step 2) [35]. These modifications produced quaternary ammonium ions that adhered to the CNC surface [49]. Furthermore, the modified CNC/CTAB reacted with the C=O group of GA to form an HC=N (step 3). After that, the terminal end of the CHO group on the CNC bound to the *C. rugosa* lipase (CRL) enzyme molecule via an imine bond (step 4). In step 5, the water molecule was desorbed and formed a CRL NH_2 group on the lipase resulting in immobilized lipase on CNC (lipase/CNC) [34].

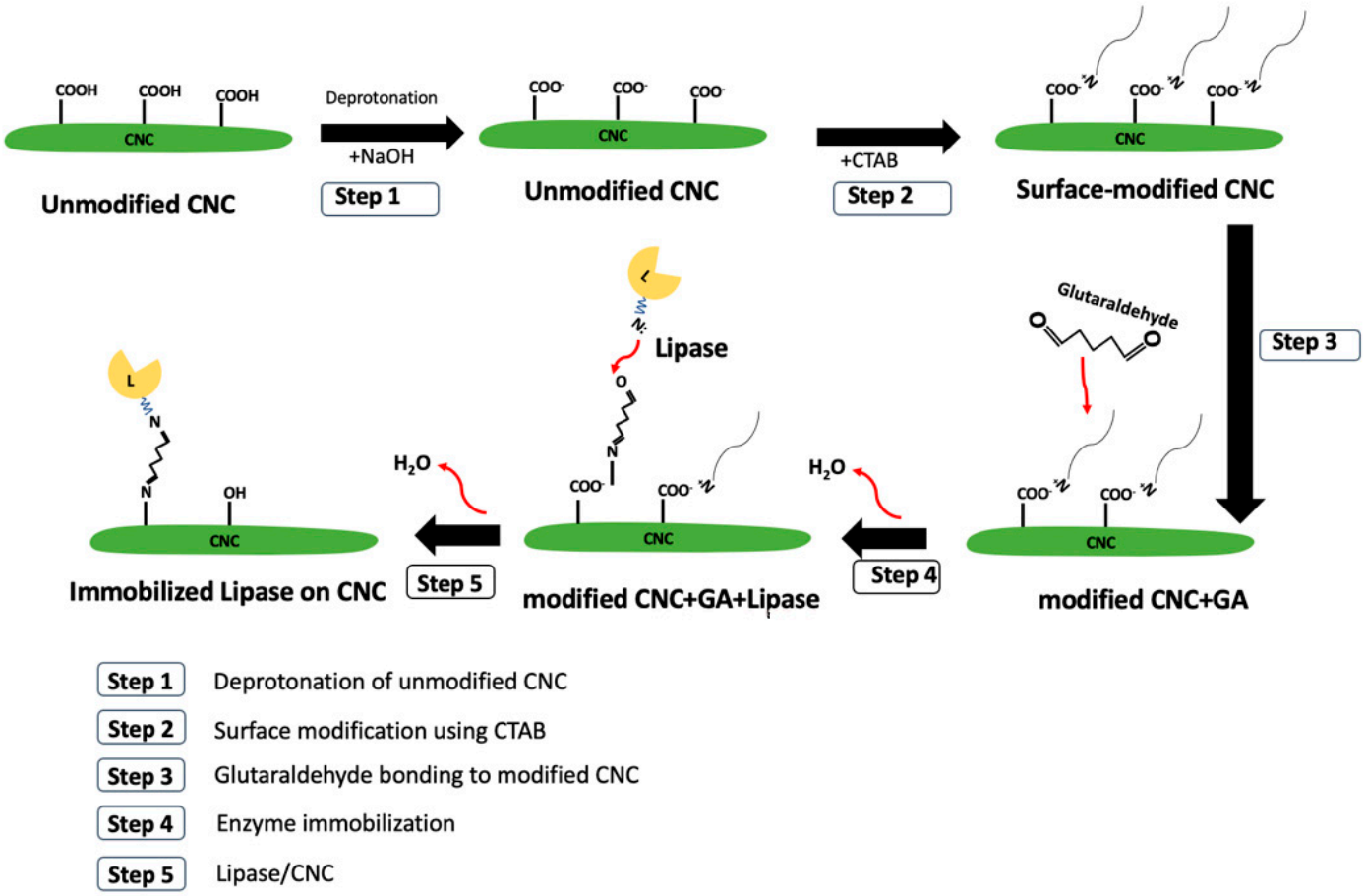

Figure 11. Scheme of the immobilized lipase onto the modified CNC.

About 88.2% of the lipase enzyme can be immobilized into the SB-20 A1-1 or RS-20 B1-1 matrix. This result is similar to a study conducted by Li et al. [22], showing the efficiency of immobilization lipase reached 84.2% using the dendrimer-polymer-modified nanoparticles as support. The results exhibit that modified CNC using CTAB on the surface can increase the enzyme loading because many functional groups of CNC can attach to the enzyme. The comparison of enzyme activity of the free enzyme and immobilized enzyme can also be seen in Table 3. As shown in Table 3, the decrease in the immobilized enzyme activity can be caused by several factors such as changes in the structure of the enzyme's active site, diffusion barriers, enzyme denaturation, and rigidification of the enzyme structure [34]. Even the immobilization efficiency shows high values; the immobilized enzyme activity is much lower compared with the free enzyme. This might be induced by the mass transfer barrier surrounding the immobilized enzyme. In addition, the results of the stability test are presented in Figure 7, indicating that the immobilized enzyme had the highest activity at 40 °C, while the free enzyme was at 30 °C. The free enzyme usually suffers at a higher temperature, leading to a decrease in its activity when the temperature increases.

According to Figure 9, the results showed that the free enzyme has greater activity than that of the immobilized enzymes, with degree hydrolysis for SB-20 A1-1 was 23% for canola oil and 12% for soyabean oil, while degree hydrolysis for RS-20 B1-1 was 30% for canola oil and 14% for soyabean oil. Free lipase and immobilized lipase showed the highest degree of hydrolysis using canola oil as a substrate. This occurrence can be caused by differences in the composition of fatty acids contained in each oil. It was previously reported that the fatty acid reactivity differs depending on the lipase source, substrate composition, water activity, solvents, etc. [50,51].

The degree of hydrolysis of canola oil using lipase RS-20 B1-1 in this study showed a lower value than that of free lipase (see Table 4). This could be due to the immobilization

efficiency (below 100%) and mass transfer in the enzymatic reaction system using the immobilized enzyme. In addition, the enzyme concentration (U/mL-substrate or U/g-substrate) used in this study is relatively small (0.75 U/mg-substrate) and can still be optimized to obtain a high degree of hydrolysis (>95%) with enzyme concentrations that are still economically feasible [30].

Repeated use of the immobilized lipase was assessed for up to three uses for the immobilized lipase SB-20 A1-1 and RS-20 B1-1, respectively (see Figure 10). Both enzymes showed enzyme activity after repeated use up to 3 times, which showed the benefits of using immobilized enzymes. The decrease in the degree of hydrolysis can be caused by enzyme loss due to the filtering process that occurs between repeated hydrolysis stages. In addition, the decrease in the degree of hydrolysis can be caused by damage to enzyme molecules by collisions between immobilized enzymes due to shaking during the hydrolysis process.

5. Conclusions

The synthesis of CNC from sugarcane bagasse and rice straw has been performed in this study by applying the oxidation method using TEMPO with modifications and various concentrations of NaOCl. NaOH pretreatment improved the crystallinity index. The CNC from sugarcane bagasse has a crystallinity index of approximately 80% with a length of 215 ± 83 nm, while the CNC from rice straw has a crystallinity index of approximately 86% with a length of 103 ± 23 nm. The use of TEMPO for the oxidation method predominantly resulted in a rod-like morphology. This CNC product exhibits good thermal stability at temperatures less than 200 °C. Moreover, the lipase was successfully immobilized in CNC from sugarcane bagasse (SB-20 A1-1) and rice straw (RS-20 B1-1) with degree hydrolysis of 23% and 30%, respectively. The immobilized enzyme has also been assessed in repeated use, which shows beneficial application compared with the free enzyme.

Author Contributions: Conceptualization, E.R. and Y.W.B.; writing—reviewing and editing; E.R., Y.W.B. and N.N.; experiments and drafting, N.T.U.C. All authors have read and agreed to the published version of the manuscript.

Funding: The financial support was under contract number 1789a/I1.C06/PL/2018 (the Asahi Glass Foundation—ITB, fiscal year 2018-2019) and Research Program ITB under contract number 139/IT1.B07.1/TA.00/2021.

Institutional Review Board Statement: Not applicable.

Informed Consent Statement: Not applicable.

Data Availability Statement: The data presented in this study are available on request from the corresponding author.

Acknowledgments: The authors would like to acknowledge Haroki Madani for assisting the schematic drawing of immobilized lipase.

Conflicts of Interest: There are no conflicts of interest to declare.

References

1. Gutiérrez-Ayesta, C.; Carelli, A.A.; Ferreira, M.L. Relation between lipase structures and their catalytic ability to hydrolyse triglycerides and phospholipids. *Enzym. Microb. Technol.* **2007**, *41*, 35–43. [CrossRef]
2. Wang, P. Nanoscale biocatalyst systems. *Curr. Opin. Biotechnol.* **2006**, *17*, 574–579. [CrossRef] [PubMed]
3. Tacias-Pascacio, V.G.; Virgen-Ortíz, J.J.; Jiménez-Pérez, M.; Yates, M.; Torrestiana-Sanchez, B.; Rosales-Quintero, A.; Fernandez-Lafuente, R. Evaluation of different lipase biocatalysts in the production of biodiesel from used cooking oil: Critical role of the immobilization support. *Fuel* **2017**, *200*, 1–10. [CrossRef]
4. Brinchi, L.; Cotana, F.; Fortunati, E.; Kenny, J.M. Production of nanocrystalline cellulose from lignocellulosic biomass: Technology and applications. *Carbohydr. Polym.* **2013**, *94*, 154–169. [CrossRef]
5. Sheltami, R.M.; Abdullah, I.; Ahmad, I.; Dufresne, A.; Kargarzadeh, H. Extraction of cellulose nanocrystals from mengkuang leaves (*Pandanus tectorius*). *Carbohydr. Polym.* **2012**, *88*, 772–779. [CrossRef]
6. Danial, W.H.; Abdul Majid, Z.; Mohd Muhid, M.N.; Triwahyono, S.; Bakar, M.B.; Ramli, Z. The reuse of wastepaper for the extraction of cellulose nanocrystals. *Carbohydr. Polym.* **2015**, *118*, 165–169. [CrossRef]

7. Zhang, K.; Sun, P.; Liu, H.; Shang, S.; Song, J.; Wang, D. Extraction and comparison of carboxylated cellulose nanocrystals from bleached sugarcane bagasse pulp using two different oxidation methods. *Carbohydr. Polym.* **2016**, *138*, 237–243. [CrossRef]
8. Budhi, Y.W.; Fakhrudin, M.; Culsum, N.T.U.; Suendo, V.; Iskandar, F. Preparation of cellulose nanocrystals from empty fruit bunch of palm oil by using phosphotungstic acid. *IOP Conf. Ser. Earth Environ. Sci.* **2018**, *105*, 12063. [CrossRef]
9. Mandal, A.; Chakrabarty, D. Isolation of nanocellulose from waste sugarcane bagasse (SCB) and its characterization. *Carbohydr. Polym.* **2011**, *86*, 1291–1299. [CrossRef]
10. Restiawaty, E.; Arabica Yatasya, F.; Ellys; Tresna Umi Culsum, N.; Akhmaloka; Wibisono Budhi, Y. Lipase immobilization onto Cellulose Nanocrystals (CNC) for catalyzing lipolysis of triglycerides. *IOP Conf. Ser. Mater. Sci. Eng.* **2021**, *1143*, 12009. [CrossRef]
11. Culsum, N.T.U.; Melinda, C.; Leman, I.; Wibowo, A.; Budhi, Y.W. Isolation and characterization of cellulose nanocrystals (CNCs) from industrial denim waste using ammonium persulfate. *Mater. Today Commun.* **2021**, *26*, 101817. [CrossRef]
12. Madani, H.; Wibowo, A.; Judawisastra, H.; Nishiyama, N.; Budhi, Y.W. One-step extraction of cellulose nanocrystals from high lignin biomass through ammonium persulfate oxidation method. *Adv. Nat. Sci. Nanosci. Nanotechnol.* **2022**, *13*, 15007. [CrossRef]
13. Hessien, M.M.; Rashad, M.M.; Zaky, R.R.; Abdel-Aal, E.A.; El-Barawy, K.A. Controlling the synthesis conditions for silica nanosphere from semi-burned rice straw. *Mater. Sci. Eng. B* **2009**, *162*, 14–21. [CrossRef]
14. Pandey, A.; Soccol, C.R.; Nigam, P.; Soccol, V.T. Biotechnological potential of agro-industrial residues. I: Sugarcane bagasse. *Bioresour. Technol.* **2000**, *74*, 69–80. [CrossRef]
15. Kim, H.J.; Park, S.; Kim, S.H.; Kim, J.H.; Yu, H.; Kim, H.J.; Yang, Y.-H.; Kan, E.; Kim, Y.H.; Lee, S.H. Biocompatible cellulose nanocrystals as supports to immobilize lipase. *J. Mol. Catal. B Enzym.* **2015**, *122*, 170–178. [CrossRef]
16. Azizi Samir, M.A.S.; Alloin, F.; Dufresne, A. Review of Recent Research into Cellulosic Whiskers, Their Properties and Their Application in Nanocomposite Field. *Biomacromolecules* **2005**, *6*, 612–626. [CrossRef]
17. Lam, E.; Male, K.B.; Chong, J.H.; Leung, A.C.W.; Luong, J.H.T. Applications of functionalized and nanoparticle-modified nanocrystalline cellulose. *Trends Biotechnol.* **2012**, *30*, 283–290. [CrossRef]
18. Zainuddin, N.; Ahmad, I.; Kargarzadeh, H.; Ramli, S. Hydrophobic kenaf nanocrystalline cellulose for the binding of curcumin. *Carbohydr. Polym.* **2017**, *163*, 261–269. [CrossRef]
19. Eyley, S.; Thielemans, W. Surface modification of cellulose nanocrystals. *Nanoscale* **2014**, *6*, 7764–7779. [CrossRef]
20. Cho, B.-N.; Chino, H.; Tsuji, H.; Kunito, T.; Makishima, H.; Uchida, H.; Matsumoto, S.; Oyaizu, H. Analysis of oil components and hydrocarbon-utilizing microorganisms during laboratory-scale bioremediation of oil-contaminated soil of Kuwait. *Chemosphere* **1997**, *35*, 1613–1621. [CrossRef]
21. Isogai, A.; Kato, Y. Preparation of Polyuronic Acid from Cellulose by TEMPO-mediated Oxidation. *Cellulose* **1998**, *5*, 153–164. [CrossRef]
22. Li, K.; Wang, J.; He, Y.; Cui, G.; Abdulrazaq, M.A.; Yan, Y. Enhancing enzyme activity and enantioselectivity of Burkholderia cepacia lipase via immobilization on melamine-glutaraldehyde dendrimer modified magnetic nanoparticles. *Chem. Eng. J.* **2018**, *351*, 258–268. [CrossRef]
23. Segal, L.; Creely, J.J.; Martin, A.E.; Conrad, C.M. An Empirical Method for Estimating the Degree of Crystallinity of Native Cellulose Using the X-Ray Diffractometer. *Text. Res. J.* **1959**, *29*, 786–794. [CrossRef]
24. Rooney, D.; Weatherley, L.R. The effect of reaction conditions upon lipase catalysed hydrolysis of high oleate sunflower oil in a stirred liquid–liquid reactor. *Process Biochem.* **2001**, *36*, 947–953. [CrossRef]
25. Fukuzumi, H.; Saito, T.; Okita, Y.; Isogai, A. Thermal stabilization of TEMPO-oxidized cellulose. *Polym. Degrad. Stab.* **2010**, *95*, 1502–1508. [CrossRef]
26. Lee, K.-Y.; Tammelin, T.; Schulfter, K.; Kiiskinen, H.; Samela, J.; Bismarck, A. High Performance Cellulose Nanocomposites: Comparing the Reinforcing Ability of Bacterial Cellulose and Nanofibrillated Cellulose. *ACS Appl. Mater. Interfaces* **2012**, *4*, 4078–4086. [CrossRef]
27. Chindaprasirt, P.; Rattanasak, U. Eco-production of silica from sugarcane bagasse ash for use as a photochromic pigment filler. *Sci. Rep.* **2020**, *10*, 9890. [CrossRef]
28. Zhang, P.; Liao, W.; Kumar, A.; Zhang, Q.; Ma, H. Characterization of sugarcane bagasse ash as a potential supplementary cementitious material: Comparison with coal combustion fly ash. *J. Clean. Prod.* **2020**, *277*, 123834. [CrossRef]
29. Avelar, M.H.M.; Cassimiro, D.M.J.; Santos, K.C.; Domingues, R.C.C.; De Castro, H.F.; Mendes, A.A. Hydrolysis of vegetable oils catalyzed by lipase extract powder from dormant castor bean seeds. *Ind. Crops Prod.* **2013**, *44*, 452–458. [CrossRef]
30. Minovska, V.; Winkelhausen, E.; Kuzmanova, S. Lipase immobilized by different techniques on various support materials applied in oil hydrolysis. *J. Serbian Chem. Soc.* **2005**, *70*, 609–624. [CrossRef]
31. Kabbashi, N.A.; Mohammed, N.I.; Alam, M.Z.; Mirghani, M.E.S. Hydrolysis of Jatropha curcas oil for biodiesel synthesis using immobilized Candida cylindracea lipase. *J. Mol. Catal. B Enzym.* **2015**, *116*, 95–100. [CrossRef]
32. Johar, N.; Ahmad, I.; Dufresne, A. Extraction, preparation and characterization of cellulose fibres and nanocrystals from rice husk. *Ind. Crops Prod.* **2012**, *37*, 93–99. [CrossRef]
33. Kumar, A.; Negi, Y.S.; Choudhary, V.; Bhardwaj, N.K. Characterization of Cellulose Nanocrystals Produced by Acid-Hydrolysis from Sugarcane Bagasse as Agro-Waste. *J. Mater. Phys. Chem.* **2014**, *2*, 1–8. [CrossRef]
34. Elias, N.; Chandren, S.; Razak, F.I.A.; Jamalis, J.; Widodo, N.; Wahab, R.A. Characterization, optimization and stability studies on Candida rugosa lipase supported on nanocellulose reinforced chitosan prepared from oil palm biomass. *Int. J. Biol. Macromol.* **2018**, *114*, 306–316. [CrossRef]

35. Ly, M.; Mekonnen, T.H. Cationic surfactant modified cellulose nanocrystals for corrosion protective nanocomposite surface coatings. *J. Ind. Eng. Chem.* **2020**, *83*, 409–420. [CrossRef]
36. Knill, C.J.; Kennedy, J.F. Degradation of cellulose under alkaline conditions. *Carbohydr. Polym.* **2003**, *51*, 281–300. [CrossRef]
37. Ciftci, D.; Flores, R.A.; Saldaña, M.D.A. Cellulose Fiber Isolation and Characterization from Sweet Blue Lupin Hull and Canola Straw. *J. Polym. Environ.* **2018**, *26*, 2773–2781. [CrossRef]
38. Elenga, R.G.; Djemia, P.; Tingaud, D.; Chauveau, T.; Maniongui, J.G.; Dirras, G. Effects of alkali treatment on the microstructure, composition, and properties of the Raffia textilis fiber. *BioResources* **2013**, *8*, 2934–2949. [CrossRef]
39. Cao, X.; Ding, B.; Yu, J.; Al-Deyab, S.S. Cellulose nanowhiskers extracted from TEMPO-oxidized jute fibers. *Carbohydr. Polym.* **2012**, *90*, 1075–1080. [CrossRef]
40. Wibowo, A.; Madani, H.; Judawisastra, H.; Restiawaty, E.; Lazarus, C.; Budhi, Y.W. An eco-friendly preparation of cellulose nano crystals from oil palm empty fruit bunches. *IOP Conf. Ser. Earth Environ. Sci.* **2018**, *105*, 012059. [CrossRef]
41. Kargarzadeh, H.; Ahmad, I.; Abdullah, I.; Dufresne, A.; Zainudin, S.Y.; Sheltami, R.M. Effects of hydrolysis conditions on the morphology, crystallinity, and thermal stability of cellulose nanocrystals extracted from kenaf bast fibers. *Cellulose* **2012**, *19*, 855–866. [CrossRef]
42. Xiang, S.; Ma, X.; Liao, S.; Shi, H.; Liu, C.; Shen, Y.; Lv, X.; Yuan, M.; Fan, G.; Huang, J.; et al. Cellulose nanocrystal surface cationization: A New Fungicide with High Activity against Phycomycetes capsici. *Molecules* **2019**, *24*, 2467. [CrossRef]
43. Nagalakshmaiah, M.; El Kissi, N.; Dufresne, A. Ionic Compatibilization of Cellulose Nanocrystals with Quaternary Ammonium Salt and Their Melt Extrusion with Polypropylene. *ACS Appl. Mater. Interfaces* **2016**, *8*, 8755–8764. [CrossRef]
44. Tong, X.; Shen, W.; Chen, X.; Jia, M.; Roux, J.-C. Preparation and mechanism analysis of morphology-controlled cellulose nanocrystals via compound enzymatic hydrolysis of eucalyptus pulp. *J. Appl. Polym. Sci.* **2020**, *137*, 48407. [CrossRef]
45. George, J.; Sabapathi, S. Cellulose nanocrystals: Synthesis, functional properties, and applications. *Nanotechnol. Sci. Appl.* **2015**, *8*, 45–54. [CrossRef] [PubMed]
46. Zhu, Y.T.; Ren, X.Y.; Liu, Y.M.; Wei, Y.; Qing, L.; Liao, X. Covalent immobilization of porcine pancreatic lipase on carboxyl-activated magnetic nanoparticles: Characterization and application for enzymatic inhibition assays. *Mater. Sci. Eng. C* **2014**, *38*, 278–285. [CrossRef]
47. Onyianta, A.J.; Dorris, M.; Williams, R.L. Aqueous morpholine pre-treatment in cellulose nanofibril (CNF) production: Comparison with carboxymethylation and TEMPO oxidisation pre-treatment methods. *Cellulose* **2018**, *25*, 1047–1064. [CrossRef]
48. Incani, V.; Danumah, C.; Boluk, Y. Nanocomposites of nanocrystalline cellulose for enzyme immobilization. *Cellulose* **2013**, *20*, 191–200. [CrossRef]
49. Moon, R.J.; Martini, A.; Nairn, J.; Simonsen, J. Youngblood, Cellulose Nanomaterials Review: Structure, Properties and Nanocomposites. *Chem. Soc. Rev.* **2011**, *40*, 3941–3994. [CrossRef]
50. Yang, T.; Xu, X.; Li, L.T. Comparison of Linoleic and Conjugated Linoleic Acids in Enzymatic Acidolysis of Tristearin. *J. Food Lipids* **2001**, *8*, 149–161. [CrossRef]
51. Karabulut, I.; Durmaz, G.; Hayaloglu, A.A. C18 Unsaturated fatty acid selectivity of lipases during the acidolysis reaction between tripalmitin and oleic, linoleic, and linolenic acids. *JAOCS J. Am. Oil Chem. Soc.* **2010**, *87*, 1301–1307. [CrossRef]